Effect of electromagnetic fields generated by Borssele export cables on harbour porpoise acoustic activity

Author(s): Stece C.V. Geelhoed, Hans Verdaat & Tony Wilkes

Wageningen University & Research report C067/22

Effect of electromagnetic fields generated by Borssele export cables on harbour porpoise acoustic activity

Authors:
Steve C.V. Geelhoed, Hans Verdaat & Tony Wilkes

Wageningen Marine Research
Den Helder, October 2022

CONFIDENTIAL no

Wageningen Marine Research report C067/22

Keywords: **Harbour porpoise, passive acoustic monitoring, electromagnetic fields.**

Client: Witteveen + Bos
Attn.: Annemiek Hermans/Just van der Endt
Leeuwenbrug 8
7400 AE, Deventer

This report can be downloaded for free from https://doi.org/10.18174/579669

Wageningen Marine Research provides no printed copies of reports

Wageningen Marine Research is ISO 9001:2015 certified.

Photo cover:

KvK nr. 09098104,
WMR BTW nr. NL 8113.83.696.B16.
Code BIC/SWIFT address: RABONL2U
IBAN code: NL 73 RABO 0373599285

A_4_3_2 V31 (2021)

Contents

Summary

Passive Acoustic Monitoring of harbour porpoise presence with ten CPODs deployed in a 500 meter spaced grid, and simultaneous measurements of EMF strength and underwater sound levels were conducted around the Borssele export cables to study if the EMF emitted by these cables has an effect on the presence of harbour porpoises during 1 September-21 October 2022. The aim of this study is to assess if there is a correlation between the EMF energy that runs through the cable, and the acoustic activity of harbour porpoises.

The acoustic activity of harbour porpoises is expressed in porpoise positive minutes (ppm), which were used as response variable for our analysis. Due to the zero-inflation in the CPOD-data (about half of the minutes had no porpoise clicks), and due to the interest in both the amount and presence of ppm, a hurdle model set was used for the analysis. Each hurdle model set consists of two statistical models:

- A presence/absence model, modelling the presence/absence of ppm.
- A non-zero model, modelling the amount of ppm, if presence of ppm is positive.

The model results showed patterns in relationships between environmental variables and the acoustic activity of harbour porpoises that reflect the results from previous studies. Taken these relationships into account, our study did not find a clear relationship between EMF and the probability of ppm, nor between wind speed and the probability of ppm.

To conclude, our study does not show a relationship between EMF emitted by the Borssele export cables and harbour porpoise acoustic activity (ppm) measured by CPODs.

1 Introduction

To transport the energy generated at the offshore windfarm Borssele to the Dutch mainland, four 220 kV high voltage export cables have been installed between the windfarm and an onshore station in Borssele. These export cables generate electromagnetic fields (EMFs) that can potentially lead to adverse effects on marine life in the vicinity of the cable. The emitted EMFs are expected to be higher for the export cables to shore compared to the inter-turbine cables, due to the amount of power being transmitted and the lower electrical capacity rating of the cables (Thomsen et al., 2015).

Currently, there is limited knowledge on the effect of EMFs on the marine ecosystem. As operator of the cables, TenneT executes a so-called Monitoring en Evaluatie Programma (MEP), to study the potential impact of EMFs on marine life. Witteveen+Bos coordinates the MEP, and has contracted WaterProof Marine Consultancy & Services BV (hereafter WaterProof) and Wageningen Marine Research (hereafter WMR) to study the potential impact of EMF on harbour porpoise, *Phocoena phocoena*. It is a protected species, and it is the most abundant marine mammal in the North Sea. The aim of this study is to assess the possible impact of electromagnetic fields generated by the Borssele export cable on harbour porpoise acoustic activity, as a proxy for the presence of harbour porpoises. More specific this study aims at answering the following question:

1. Is there a correlation between the EMF energy that runs through the cable, and the acoustic activity of harbour porpoises?

Harbour porpoise presence was studied with a Passive Acoustic Monitoring (PAM) network around the Borssele export cable, whilst simultaneous measurements by Waterproof provided information on EMF and underwater sound. The environmental measurements, EMF strength above the export cables and sound levels in the PAM study area, are described by Van der Neut & Brinkkemper (2022). This report describes the PAM results and aims at elucidating if the export cables had an effect on the presence of harbour porpoises.

2 Materials and Methods

2.1 Study area

As described by Van der Neut & Brinkkemper (2022) an area close to the Borssele OWF was selected to conduct noise measurements and passive acoustic monitoring of harbour porpoise presence (*Figure **1***). At this location, ship traffic intensity is relatively low (see AIS data in *Figure **1***) and it is expected that possible effects of the EMF strength on harbour porpoise behaviour is therefore easier to isolate from effects due to high sound exposure levels.

Ten measurement stations were deployed in a 500 meter spaced grid around the cable, extending in a south-westerly direction, as environmental conditions in this direction are relatively homogenous. Harbour porpoise acoustic activity was measured at these ten stations using so-called CPODs, whilst sound levels were measured at stations 2 and 10 only (*Figure **1***). Four cardinal marker buoys (yellow triangles) were placed around the measurement stations by the Rijksrederij for safety reasons, and to avoid loss of equipment due to bottom trawling.

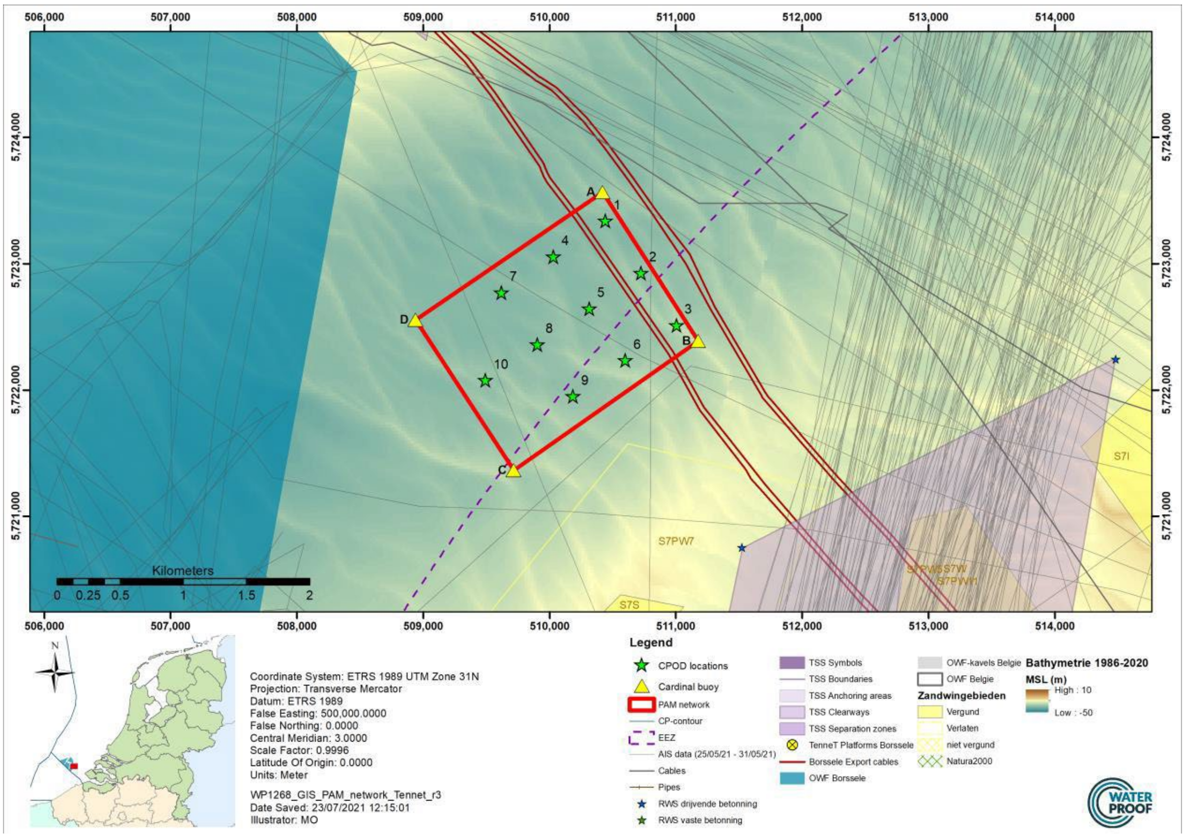

Figure 1. Study area. The study area is delineated with a red rectangle. CPOD-locations are indicated with a green star. Cardinal marker buoys on the corners of the study area are indicated with a yellow triangle.

2.2 Passive acoustic monitoring

Passive acoustic monitoring of harbour porpoises was conducted with CPODs. A CPOD, or Continuous POrpoise Detector (Chelonia Ltd., U.K.), is a device that consists of a polypropylene casing with the hydrophone housing at one end and a removable lid at the other end (*Figure* ***2***). A metal retaining ring around the centre of the CPOD holds the mooring line. Two lines are attached to the anchor. The housing contains an amplifier, a digital waveform analyser, a data-logger that logs echolocation click-activity, and 10 D-cell batteries; the CPOD has a positive buoyancy of approximately 0.7 kg. The data are stored

Figure 2. A CPOD. Photo Hans Verdaat

on a Secure Digital (SD) flash card and later analysed on a PC to identify the presence of harbour porpoises by detecting the trains of ultrasonic echo-location clicks they produce. To minimize data storage requirements a summary of the click features is logged, comprising time, duration, dominant frequency, bandwidth and amplitude. Furthermore information on angle of the CPOD and temperature was stored.

A CPOD relies on the distinctive nature of porpoise echolocation signals that last 50-150 microseconds, and contain virtually no energy below 100 kHz. The main part of the energy is in a narrow band between 120-150 kHz, peaking around 132 kHz (Au et al., 1999). Detection of these so-called harbour porpoise clicks is basically done by a comparison of the energy of the acoustic signal in a small band around a high and a low frequency, the so-called A- and B-filter. Acoustic signals that have substantially more energy in the A-filter are probably emitted by a harbour porpoise. By analysing the time intervals between successive clicks, harbour porpoise click trains can be recognised by a gradual change of click intervals and amplitudes. For this study, the A-filter frequency was set at 100 kHz and the B-filter frequency was set to 80 kHz. The train quality filter was set to record Hi(gh) and Mod(erate) quality click trains from porpoise-like clicks and dolphin clicks. This setting filters out click trains of low quality and thus reduces the number of false detections.

Before the CPODs were deployed in the study area, all devices were calibrated by the German Oceanographic Museum (Meeresmuseum, Stralsund). This calibration ensures that all devices perform as expected and yield results that are directly comparable between the different locations. The German Oceanographic Museum has developed a standard calibration for the CPODs according to guidelines from the international AMPOD-project that aimed at standardization of acoustic measurements (Verfuß et al., 2010).

Each individual CPOD was tested in a tank at the museum to quantify it's sensitivity, using calibrated Reson TC 4013 hydrophones as transmitter and receiver. The transmitter sent out acoustic signals at different frequencies that were measured by the calibrated hydrophone. This hydrophone was replaced by a CPOD that was exposed to the same calibration signals from the transmitter. The same procedure was repeated for different positions along the CPODs horizontal axis in order to measure directional variation. The sensitivity of a CPOD was compared to the received levels and mean peak-to-peak pressures (Ppp) of the calibrated hydrophones. Detection thresholds and the relationship between receiving level and the corresponding Ppp-values for each CPOD were calculated with two methods: 50%-detection thresholds and linear regression models. Details of these calculations and the calibration method can be found in Verfuß et al. (2010).

For the calibrations, the received levels of mean peak-to-peak pressures emitted frequencies of 100, 110, 120, 130 and 140 kHz were measured for each individual CPOD. Since the main part of the energy of a porpoise click is around 132 kHz the differences at 130 kHz are the most applicable for comparison. The highest variation in peak-to-peak pressure at 130 kHz lies between 110 and 120 dB re µ1Pa for most PODs. This difference in peak-to-peak pressure corresponds to a difference in received sound level of less than 3 dB. Only CPODs that operate within the maximum accepted variation recommended by the AMPOD-project (Verfuß et al., 2010) were used.

2.3 Data preparation

CPODs were deployed in the study area on 1 September 2021 and recovered 28 October 2021. After recovery of the CPODs, data were downloaded and processed with the software "CPOD.exe" version 2.044 (Chelonia Ltd). Since CPODs cannot record real time, the date and activation time of the CPOD were assigned to the so-called CP1-files when downloading these files from the SD card. To validate the data the files were checked visually; a first cross-check was made to ensure the times thatwere recorded during deployment and retrieval correspond with the times in the CP1-file: CPOD activated, CPOD submerged, CPOD surfaced, and CPOD deactivated. Each file was truncated at the start and end to delete erroneous data, due to handling of the CPOD. A sample of the data-files has been screened for errors by visually checking graphs for unexpected transitions or gaps in parameters like click frequency, CPOD angle, and temperature measured by the CPOD.

Data were further processed and checked for errors. First, classification of click trains was applied using the KERNO classifier from the "CPOD.exe" software, yielding *.CP3 files. These files contain information on the number of harbour porpoise echolocation clicks per minute. This consists of many zero observations (minutes without porpoise clicks), as well as porpoise positive minutes (ppm).

The CPODs are arranged in four groups:

- group 1 consists of CPODs 1, 2, and 3, and are in between and parallel to the two TenneT electricity cables.
- group 2 consists of CPODs 4, 5, and 6, and to the South-West of both cables, also parallel to the cables.
- group 3 consists of CPODs 7, 8, and 9, and are parallel to and South-West of group 2.
- group 4 consists of CPOD number 10, which is the most South-West and thus farthest away from the TenneT cables.

Sound measurements were available from 1 September 2021 until 21 October 2021. The Sound data contains the average unweighted, broadband Sound Pressure Level (SPL) in dB re 1 μPa · s, as well as the 50%, 95% and 100% quantiles of the SPL. It also contains these values for the vhf-weighted SPL to account for the hearing sensitivity of harbour porpoises (cf Dekeling et al, 2014; Tougaard et al, 2015). The broadband SPL is weighted by the audiogram for cetaceans with very high frequency (vhf) hearing sensitivity. Both SPL-values are recorded every minute (see Van der Neut & Brinkkemper (2022) for details).

The Energy data contains the Electro Magnetic Field (EMF, measured in micro Tesla) measurements close to the shore. We assume that the EMF is the same across the entire length of the two cables (see Van der Neut & Brinkkemper (2022) for details).
Weather data from KNMI station 313 Vlakte van de Raan, closest to our study area, contain the wind information. The hourly-average wind speed ("FH," in 0.1 m/s) and the wind direction ("DD", in 360 degree angle) were used in this study (the other wind measurements were highly correlated). For some observations, wind direction was zero, meaning a windless moment(<0.1% of the data). These observations were excluded from the analysis.
Finally, the distance of the moon from the sun for each observation in the data was estimated based on the date of each observation, using the lunar R-package (Lazaridis, 2014).

2.4 Data analysis

We used data from 1 September 2021 until 21 October 2021 for the statistical analysis, since sound measurements were restricted to this period. Although we are interested in answering the following question:

- Is there a correlation between the EMF energy that runs through the cable, and the acoustic activity of harbour porpoises?

It is necessary to answer a second question, since the strength of EMF is highly correlated with the wind speed:

- Is there a correlation between the wind speed, and the acoustic activity of harbour porpoises?

The correlation between EMF and wind speed does not allow to analyse both in one model.
The acoustic activity of harbour porpoises is expressed in porpoise positive minutes (ppm), which were used as response variable for our analysis. Due to the zero-inflation in the CPOD-data (about half of the minutes had no porpoise clicks), and due to the interest in both the amount and presence of ppm, a hurdle model set was used for both the EMF analysis, and for the wind analysis. Each hurdle model set consists of two statistical models:

- A presence/absence model, modelling the presence/absence of ppm.
- A non-zero model, modelling the amount of ppm, if presence of ppm is positive (i.e. ppm>0).

For the presence/absence model, a Bernoulli Generalized Additive Model (GAM) with logit-link function was used. For the non-zero model, a Gamma Generalized Additive Model with log-link function and offset term was used. This GAM-approach takes different sources of variation such as location and hour of the day, and environmental covariates such as lunar cycle, wind speed, sound exposure etc. into account in describing harbour porpoise acoustic activity. Including EMF makes it possible to describe its relationship with harbour porpoise acoustic activity, given the variation in ppm due to the forementioned sources and covariates.
The non-zero model has some additional complexity that is explained in the next paragraphs. The non-zero model describes the relation between different parameters and ppm, expressed as y. The ppm cannot be higher than 60, as there are 60 minutes in an hour. The proportion of the non-zero positive minutes can be expressed as follows:

$$y_{\text{prop}} = \frac{y_{y>0}}{60}$$

where $y_{y>0}$ are non-zero ppm's. This proportion is not a true probability, because it is a proportion of time (so no counting process is present). Furthermore, its distribution is right skewed. For these reasons the Gamma distribution was chosen for the model. The response was re-defined to be a strictly positive ratio instead of a proportion, as follows:

$$y_{\text{ratio}} = \frac{y_{y>0}}{60 - y_{y>0}}$$

As a Gamma model with log-link function is used, the relation between the linear predictors η and the response is as follows:

$$\log\left(\frac{E(y_{y>0})}{60 - y_{y>0}}\right) = \eta$$

This can then be re-formulated as:

$$\log\left(E(y_{y>0})\right) = \eta + \log(60 - y_{y>0})$$

Thus $\log(60 - y_{y>0})$ is the offset term.
Fitted values for use in the residuals and diagnostic plots are computed by making predictions while including this offset term. Predicting the ratio $\frac{y_{y>0}}{60-y_{y>0}}$ is computed by leaving out the offset term. Predicting the actual porpoise positive minutes, is done as follows:

$$E(y|y > 0) = \frac{E(y_{\text{ratio}})}{1 + E(y_{\text{ratio}})} \times 60$$

where $E(y_{\text{ratio}})$) are the predictions from the Gamma model without the offset term (i.e. replacing the offset term with 0).

2.5 Model formulations

The used models can be formulated as follows.
for the EMF based models:

$$\text{logit}\left(P(y > 0)\right) = \text{smoothers} + \text{locationgroup*EMF}$$
$$\log\left(E(y|y > 0)\right) = \text{smoothers} + \text{locationgroup*EMF}$$

for wind based models:

$$\text{logit}\left(P(y > 0)\right) = \text{smoothers} + f_{\text{cat}}(\text{location group}) + s(\text{FH})$$
$$\log\left(E(y|y > 0)\right) = \text{smoothers} + f_{\text{cat}}(\text{location group}) + s(\text{FH})$$

The response variable ppm is expressed as y. In the above formulations, f_{cat} stands for the function of a categorical covariate.

The term smoothers represent the following:

$$cc_0^{23}(\text{hour}) + cc_1^{360}(\text{DD}) + s(\text{SPL\_vhf}) + s(\text{SPL\_broadband}) + s(\text{lunar.dist})$$

with $s(\ )$ being the low-rank thin-plate smoother function with mgcv's default parameters (see Wood 2011, 2013 & 2017), and $cc_a^b(\ )$ being a cyclic cubic regression spline with boundary knots a and b. These smoothers were applied to the following covariates:

- hour: the hour of the day (0-23)
- DD: the wind direction, in angle degrees (360=North; 90=East; 180=South; 270=West)
- SPL_vhf: the vhf-weighted SPL
- SPL_broadband: the unweighted SPL
- lunar.dist: the distance between the moon and the earth, measured in the number of earth radii

The hour and wind direction (DD) covariates were entered in the models as cyclic cubic regression splines. The lunar distance and both SPL covariates were implemented in the models as low-rank thin-plate smoothers.
In all models, location group was a fixed effect. As there was only one categorical fixed effect in all models, no intercept term was included in the model, to aid (visual) interpretation.
In the EMF based models, the EMF Total covariate was implemented as a third degree b-spline (Ramsay, 1988; Wegman & Wright, 1983) with a single knot at 2, boundary knots at 0 and 5.5204, and no intercept knot. This spline was entered solely as an interaction term with location group (the main effect would not make sense, since all categories of location group were given a coefficient; no reference level and no intercept was implemented). In the wind based models, the FH covariate was implemented as a low-rank thin-plate smoother.

The term locationgroup*EMF represents the following:

$$f_{\text{cat}}(\text{location group}) + f_{\text{cat}}(\text{location group}) \times bs(\text{EMF})$$

where bs stands for the B-spline (including its coefficients) with the parameters described earlier.

To compare the models AIC (Sakamoto et al., 1986), BIC diagnostics (Schwarz, 1978 see *Table **2***), the model fit (*Table **1***), and the confidence interval width of the main effects were used. No violations of the model assumptions were found in the diagnostic plots for the Bernoulli models. For the Gamma models, some slight heteroskedasticity was found, but not serious enough to be a real issue (see for instance Wikipedia https://en.wikipedia.org/wiki/Homoscedasticity_and_heteroscedasticity).

3 Results

3.1 Acoustic activity of harbour porpoises

Acoustic activity of harbour porpoises, i.c. porpoise clicks, was detected on all locations. Based on the number of porpoise clicks the indicator ppm (porpoise positive minute) was calculated on an hourly basis, and visualized in Figure 3. for each location. Porpoise clicks were not only detected on all locations, but they were detected during the whole study period on each location as well. Boxplots summarize the acoustic activity of harbour porpoises for each location (*Figure 4*), showing that porpoise acoustic activity was low with <10 ppm/hr.

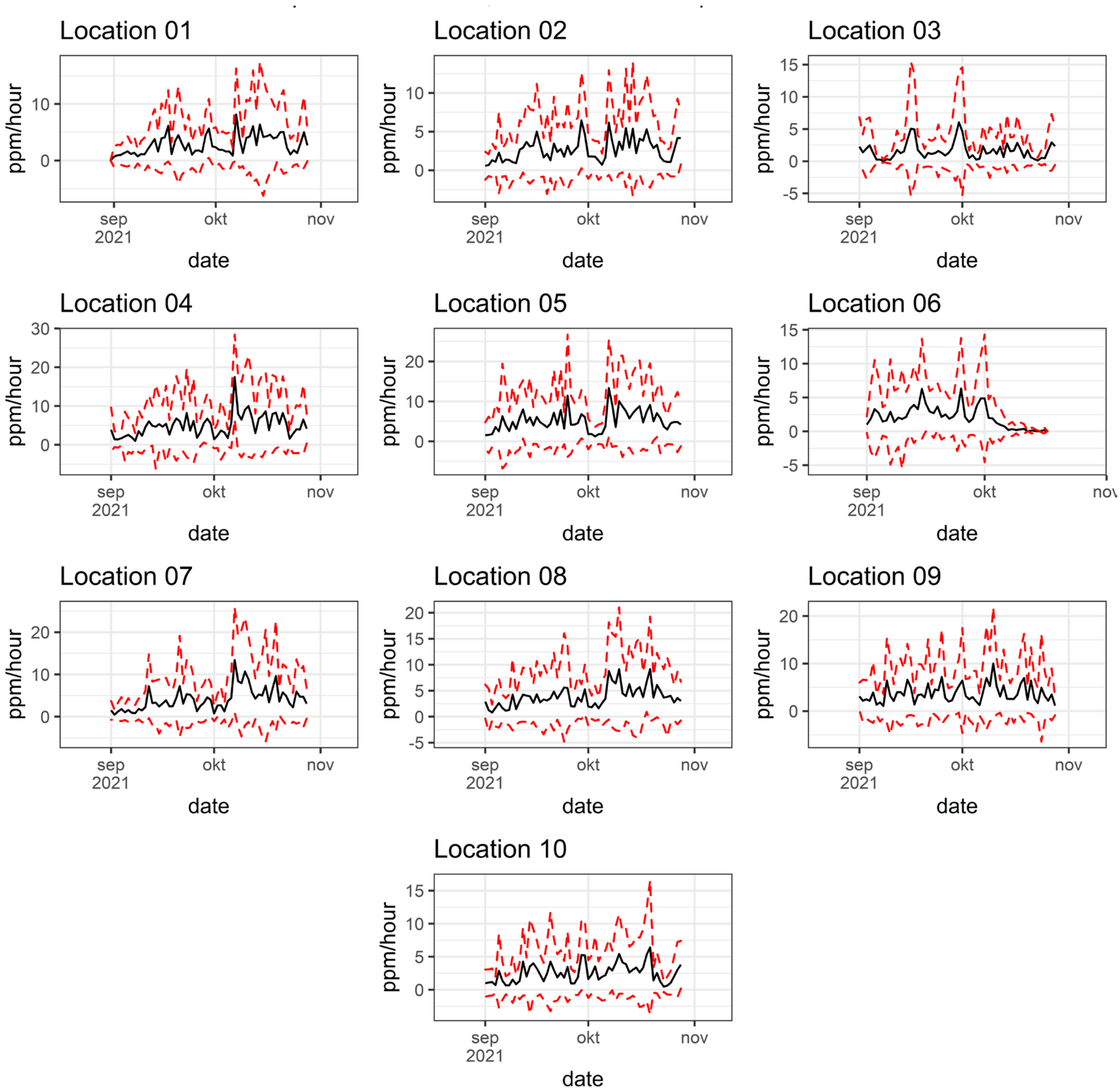

Figure 3. Harbour porpoise activity per location, expressed as daily ppm/hr. Note that the maximum daily ppm/hr is 60. Black solid lines represent the mean, red dashed lines represent the standard deviation.

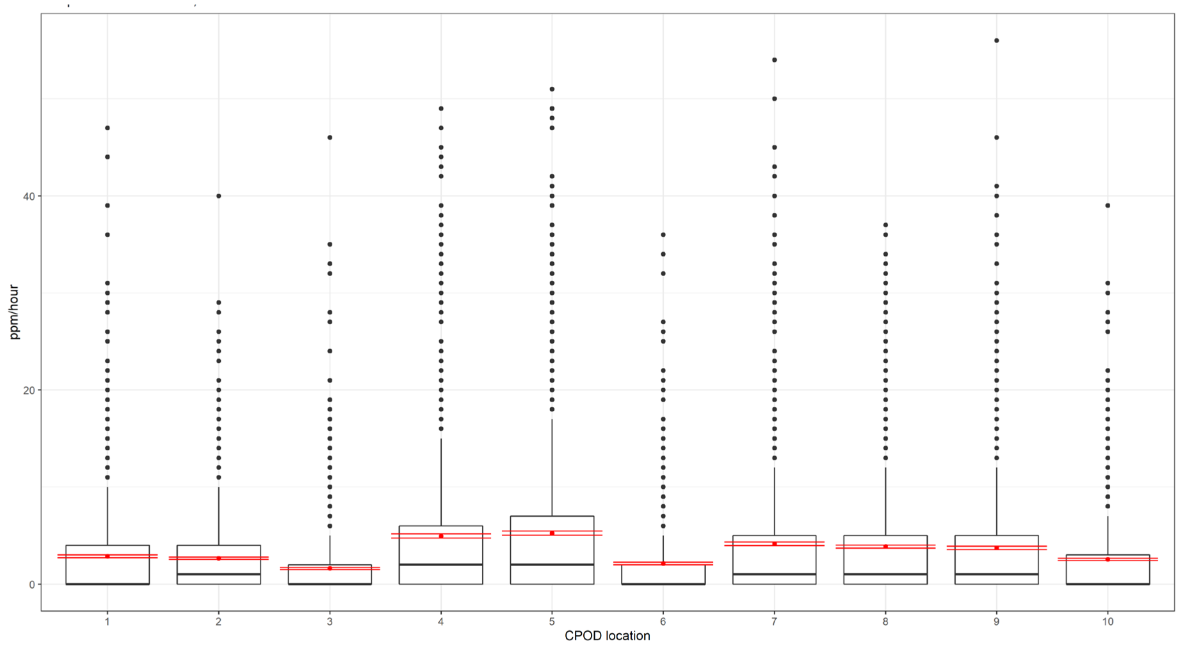

Figure 4. Harbour porpoise acoustic activity per location, expressed as daily ppm/hr. Note that the maximum daily ppm/hr is 60. The red dot represents the mean, the red bars show the standard deviation.

3.2 EMF-based models

The results of the EMF-based whole hurdle model are presented as predictor effect plots in *Figure 5*, the plots show the relationship between a covariate and the predicted ppm, with all other covariates fixed at their mean value. The shape of the relation and therefore the relative effect of the covariate on the predicted ppm value, will not change if other fixed values are chosen. The results of the underlying presence/absence and non-zero models are presented in Appendix: EMF-based coefficient plots.

The predictor effect plots show the following patterns in the other (than EMF) covariates, set B in *Figure 5*. Hour of the day shows a small dip in ppm around midday (13 o'clock), and a small peak in the evening. Wind direction (DD) does not show a relationship with ppm, although there is a higher expected ppm with near-northerly winds (ca 360 degrees), and a lower expected ppm with south-easterly winds (ca 40 degrees). A slightly decreasing but not definitive relationship can be seen between lunar distance and the expected value of ppm. Sound exposure shows a decrease in the expected value of ppm as the vhf-weighted SPL increases. This relationship was found to be significant, and nearly linear. The relationship between the unweighted broadband SPL and ppm was found to be nearly completely flat.

The relationship between EMF and ppm for the different location groups (set A in *Figure 5*) was inconsistent and mostly flat. In other words, the predicted ppm did neither go consistently up or down as EMF increases, nor showed a decrease above a certain EMF level.

3.3 Wind-based models

The results of the wind-based whole hurdle model are presented as predictor effect plots in *Figure 6*. The results of the underlying presence/absence and non-zero models are presented in Appendix: wind-based coefficient plots.

The predictor effect plots (*Figure 6Figure 6*) show the same patterns in the covariates Hour of the day, wind direction, lunar distance, vhf-weighted SPL and unweighted broadband SPL as in the EMF-based whole hurdle model (*Figure 5*)*Figure **5***). No clear relationship was found between wind force (FH) and the predicted ppm. Location group, however, showed clear differences, with lower predicted ppm in the location groups 1 and 4, whilst the two groups between the cable and the furthest CPOD-location showed higher predicted ppm's.

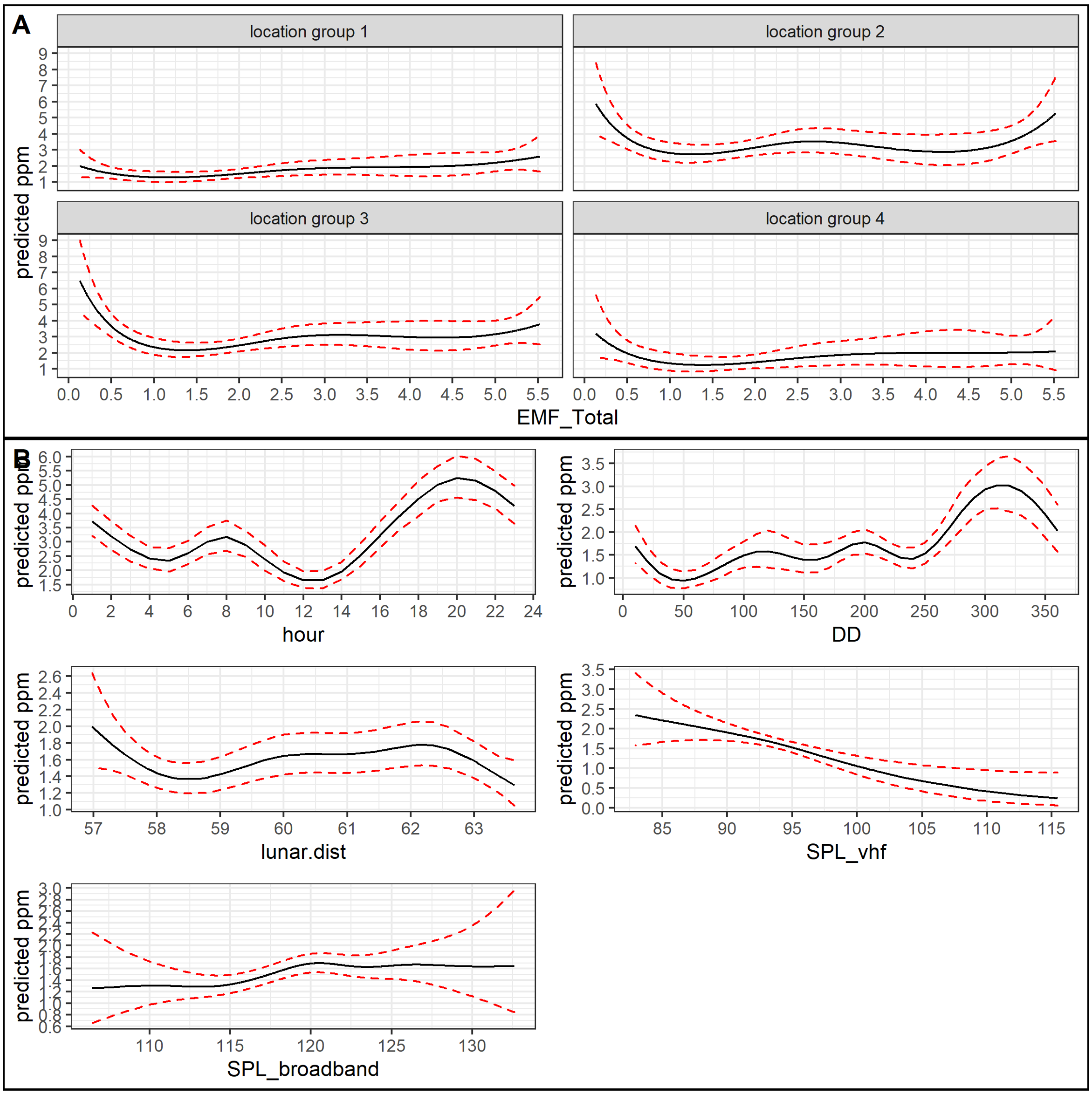

*Figure 5. Predictor effect plots for the EMF based whole hurdle model set. In each plot, only the term(s) of interest vary, while all covariates are fixed at their mean values. See pp 10 for a description of the covariates. For plots that do not involve the location groups, the location group was set to 1. The solid line represents the expected value of the predictions, and the red dashed lines indicate the 95% confidence interval. There are 2 sets of plots shown here. Set A shows the main covariates (EMF*locationgroup), and set B the other covariates.*

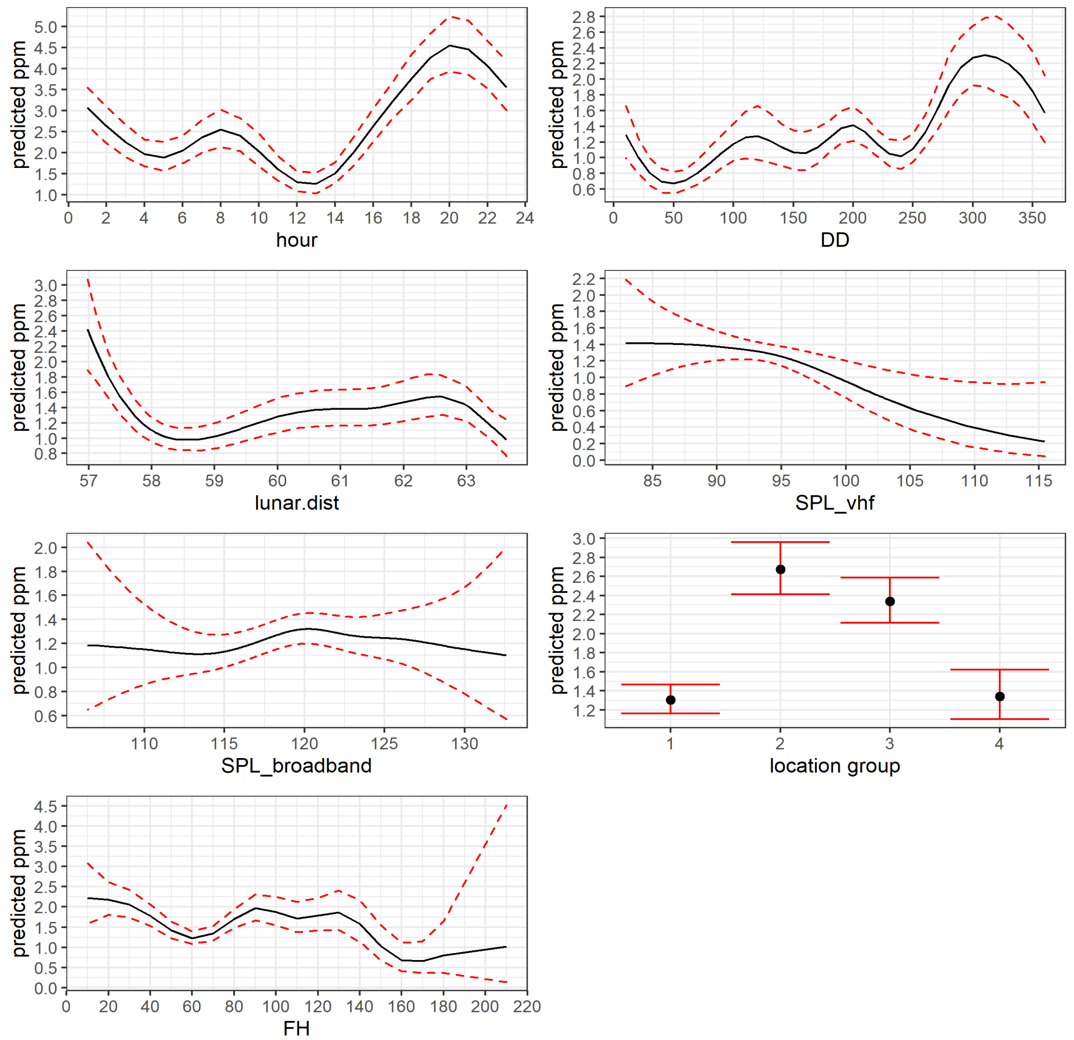

Figure 6. Predictor effect plots for the wind based whole hurdle model set. In each plot, only the term(s) of interest vary, while all covariates are fixed at their mean values. See pp 10 for a description of the covariates. For plots that do not involve the location groups, the location group was set to 1. The solid line represents the expected value of the predictions, and the red dashed lines indicate the 95% confidence interval.

The wind-based hurdle model has a very slightly better fit than the EMF-based hurdle model (see *Table 1*). The AIC and BIC information criteria values of the models are relatively close to each other, and thus inconclusive whether the EMF- or wind-based hurdle models describe acoustic activity of harbour porpoises the best (see *Table 2*).

Table 1. Fit of the EMF- and wind-based models. The closer the fit slope is to 1, the better the model predictions are. The closer the MAD to 0, the better. MAD and fit slope are both non-negative numbers (no upper bound). The 0/1 loss can take any value between 0 and 1; the closer to 0, the better.

Model	MAD	0/1-loss	fit slope
EMF	4.094121	0.4596873	0.6854507
Wind	4.082747	0.4596873	0.7086152

Table 2. The Information Criteria of the EMF- and wind-based models.

Model Set	Model Part	AIC	BIC
EMF	Bernoulli	15,114.80	15,461.80
Wind	Bernoulli	15,079.29	15,392.38
EMF	Gamma	231,227.20	231,542.23
Wind	Gamma	235,990.69	236,251.18

4 Discussion

In our PAM study we used acoustic activity of harbour porpoise, expressed as porpoise positive minutes, as a proxy for porpoise presence. We assume that the detection probability of harbour porpoise clicks and false alarm rate are constant, or at least not skewed in relation to environmental factors. The assumption to use ppm as a proxy for harbour porpoise presence is based on studies on acoustic behaviour of harbour porpoises at sea that concluded these animals use echolocation almost continuously (Teilmann *et al*., 2005. Verfuß *et al*., 2005). PAM, however, inherently has one major limitation. PAM lacks information to derive absolute numbers of individual porpoises from the acoustic detections (see Scheidat *et al*, 2019 for a review), therefore acoustic detections of porpoise clicks can only be used as a proxy for harbour porpoise presence.
Differences in the surroundings or behavioural changes were reflected in changes in click intensity and did not result in long interruptions of echolocation. Ongoing work in Danish waters, however, demonstrated the existence of potential sleeping periods, characterized by a reduced acoustic activity (Wright *et al*., 2013). Furthermore disturbance, by ship noise, has been shown to potentially reduce acoustic activity (Wisniewska *et al*., 2018). All in all, harbour porpoises can reduce their acoustic activity in specific conditions. Most researchers, however, assume that general patterns found by PAM studies are not affected by these reductions.

PAM studies in offshore wind farms on the Dutch Continental Shelf (Geelhoed *et al.*, 2018; Scheidat *et al.,* 2011; Van Polanen Petel *et al.,* 2012), and a study between the island of Borkum into the Eems-Dollard estuary (Brasseur *et al.*, 2010) show similar seasonal patterns, with strong daily and hourly variations in acoustic activity of harbour porpoises. Although our study period is less than two months our results confirm this strong variation.
This study showed patterns in relationships between environmental variables and ppm that confirm the results from previous studies. The daily pattern in acoustic activity we found, with a lower probability of ppm during the day and a higher probability during the (first part of the) night, was found from northern Scotland (Williamson *et al.*, 2017), in Danish and German North Sea waters (Carlström, 2005; Schaffeld *et al*., 2016; Teilmann *et al*., 2013) to the Wadden Sea (Zein *et al.,* 2019). Superimposed on these daily rhythms, several studies found moon-related tidal patterns (e.g. IJsseldijk *et al*., 2015). Our study period was less than two lunar cycles, and therefore might be too short to confirm this pattern.

The effect of sound on porpoise acoustic activity that we found, is in line with a recent analysis of harbour porpoise activity and sound in the Borssele wind farms: De Jong *et al.* (in prep) found an almost linear relationship between an increase in vhf-weighted SPL and a decrease in the probability of ppm, whereas they also found a less clear relationship with the unweighted broadband SPL. This lack of a relationship is likely caused by the low-frequency sound in the unweighted broadband SPL, which harbour porpoise cannot hear.
All in all, taken the forementioned relationships between the different covariates and the acoustic activity of harbour porpoises into account, we did not find a clear relationship between EMF and the probability of ppm, nor between wind speed and the probability of ppm. Although the CPODs closest to the export cables showed lower ppm's than the two location groups further away from the cables, the most distant CPOD showed similar ppm's. Wind speed and EMF are strongly correlated, therefore they cannot be included in one model. Since wind speed has been shown to have an effect on the probability of ppm (e.g. Geelhoed et al., 2018; de Jong et al. in prep) and the wind-based model performs slightly better than the EMF-based model, we choose to include the results of the wind-based model in this report.

The sensitivity of a harbour porpoise to EMF depends on its ability to detect the electromagnetic radiation and the impact the EMF has on an individual porpoise. In general, a stimulus, i.c. EMF, is detectable if it exceeds a species-specific sensory threshold. Detection by an animal does not necessarily has any influence on the animal. Higher EMF intensities can potentially affect an animal, both positive or negative. Analogue to the categorization in different impact zones of sound on marine mammals (Richardson et al., 1995) we can define the following zones for EMF:

1. *Zone of detectability*. In this zone the EMF will be detectable by the marine animal.
2. *Zone of masking*. In this region the EMF interferes with the animal's ability to perceive relevant electromagnetic stimuli.
3. *Zone of avoidance or attraction*. The region where EMF induced behavioural changes are likely to occur in marine animals, such as swimming away from the source to avoid the EMF exposure, or swimming towards the EMF source.
4. *Zone of injury*. The region where EMF induced physical damages are likely to occur.

Although EMF intensity diminishes further away from the source, it should be noted that EMF radiation has a limited range (<20 m, Hutchison et al. 2020a). Subsequently the impact zones are small, and boundaries between them difficult to establish.
Studies on EMF and marine species are scarce, but show that fish species, especially elasmobranches and diadromous species like eels and salmonids, are sensitive to electromagnetic fields, whilst sensitivity in marine mammals is poorly understood (Gill et al., 2014). Hutchison et al. (2020b) suggest that marine species are sensitive to low intensity magnetic fields (nano (η) or micro (μ) Tesla), and are able to detect small changes in the global magnetic field (25-65μT). Measurements to quantify the zone of detectability are lacking, but Tricas & Carlson (2012) suggests that the harbour porpoise can detect magnetic fields above 0.05μT. They did not describe above which level effects could occur, nor did they explain how this value was established. In a review, Kirschvink (1990) found a relation between marine mammal strandings and an increase in EMF intensity of 1% relative to the Earth's magnetic field, which amounts to 0.05μT in the North Sea.

In our study measured EMF strength reached a maximum of 5.5 μT (Van der Neut & Brinkkemper, 2022), but our results did not show a relationship between ppm and EMF. We cannot exclude that harbour porpoises detected the EMF from the export cables, nor can we exclude that a behavioural response occurred closer to the cable. The overall acoustic activity of porpoises in the study area was low (< 10 ppm/hr), which made an analysis of feeding buzzes as proxy for feeding behaviour impossible. The ratio between feeding buzzes and acoustic porpoise detections typically is ca 0.25 (Berges et al., 2019), which means the amount of detected feeding buzzes is in the order of magnitude of tens per location, too low for a GAM analysis.

5 Conclusions and recommendations

The current study is one of the first to investigate the effect of EMF on harbour porpoises. Our study does not show a relationship between EMF emitted by the Borssele export cables and harbour porpoise acoustic activity measured by CPODs. Our study, however, was conducted in a small area (ca 1.5x2 km) during a short time period (1 Sep-21 Oct). Furthermore, the effect distance of the EMF-emitting cables is expected to be less than 20 m, rendering it even more challenging to measure an effect.

Further research on the potential effect of EMF on harbour porpoises under different environmental conditions or during other times of the year (in the porpoise yearly cycle) could provide a firmer basis to exclude effects. For such a research we recommend conducting a PAM study similar to ours, with an adjusted setup to measure acoustic activity of harbour porpoises on one row of CPODs near or, if possible, between the cables and one row on both sides parallel to the cables, in order to decrease the distance between the measuring locations and the EMF-source.

Since PAM studies ‘only’ result in acoustics detections of harbour porpoises as proxy for their presence other methods to study porpoises can potentially obtain additional and more detailed data. If a follow-up with future studies is decided upon to further elucidate the potential effect of EMF on harbour porpoises, we recommend considering research on the behaviour of ‘individual’ harbour porpoises and their reaction to the cables. This can be done by tracking animals. Methods to track porpoises are tagging of animals (see Scheidat et al., 2016; Vrooman et al., 2022 for a review) or acoustically detecting animals by arrays with multiple synchronized hydrophones (see Scheidat et al., 2019 for a review).

Tagging can provide information on the behaviour of individual harbour porpoises. Archival tags, containing different sensors (e.g. EMF), can be instrumental in collecting data on dive patterns, swimming speed or other behaviour, providing data to compare in different conditions. A pilot to tag porpoises in Dutch waters is about to start within a year. In the pilot porpoises from rehabilitation that will be released in the North Sea will first be tagged. In the future possibilities to catch and tag porpoises at sea will be explored (Vrooman et al., 2022). If the latter succeeds, however. the chance to tag animals with relevant sensors that swim in vicinity of EMF is very small. Tagging of harbour porpoises to collect data on effects of EMF seems not feasible at the moment.

The second option to track porpoises by means of acoustic arrays consisting of multiple hydrophones seems more feasible, but is challenging as well. *"The relatively high attenuation and directionality of NBHF clicks makes the harbour porpoise a particularly poor candidate species for localisation using PAM."* (Macaulay *et al,.* 2017). Recently, some progress has been made in the development of these arrays; some manufacturers offer custom-made harbour porpoise tracking devices now. These devices can potentially be used to track porpoises in a small area, but successful field studies are not yet conducted.

To conclude, our study is a first pilot to measure effects of EMF on harbour porpoises, and did not find effects. Further research building on our approach can provide a firmer basis to verify or falsify our results.

6 Quality Assurance

Wageningen Marine Research utilises an ISO 9001:2015 certified quality management system. The organisation has been certified since 27 February 2001. The certification was issued by DNV.

References

Au, W.W.L., Kastelein, R.A., Rippe, T. & Schooneman, N.M., 1999. Transmission beam pattern and echolocation signals of a harbor porpoise (*Phocoena phocoena*). Journal of the Acoustical Society of America 106(6): 3699-3705.

Allaire, J., Xie, Y., McPherson, J., Luraschi, J., Ushey, K., Atkins, A., … Iannone, R., 2019. Rmarkdown: Dynamic documents for r. Retrieved from https://github.com/rstudio/rmarkdown

Berges, B.P.J., Geelhoed, S.C.V., Scheidat, M. & Tougaard, J., 2019. Quantifying harbour porpoise foraging behaviour in CPOD data: identification, automatic detection and potential application. Wageningen Marine Research report; No. C039/19. Wageningen Marine Research. https://doi.org/10.18174/475270

Brasseur, S., Aarts, G., Bravo Rebolledo, E., Cremer, J., Fey-Hofstede, F., Geelhoed, S., Lindeboom, H., Lucke, K., Machiels, M., Meesters, E., Scholl, M., Teal, L. & Witte, R., 2011. Zeezoogdieren in de Eems; studie naar de effecten van bouwactiviteiten van GSP, RWE en NUON in de Eemshaven in 2010. Rapport C102a/11. Wageningen IMARES.

Carlström, J., 2005. Diel variation in echolocation behavior of wild harbor porpoises. Marine Mammal Science 21: 1-12.

Dekeling, R.P.A., Tasker, M.L., Graaf, A.J. van der, Ainslie, M.A., Andersson, M.H., André, M., Borsani, J.F., Brensing, K., Castellote, M., Cronin, D., Dalen, J., Folegot, T., Leaper, R., Pajala, J., Redman, P., Robinson, S.P., Sigray, P., Sutton, G., Thomsen, F., Werner, S., Wittekind, D. & Young, J.V., 2014. Monitoring Guidance for Underwater Noise in European Seas, Part III: Background Information and Annexes, JRC Scientific and Policy Report EUR 26556 EN, Publications Office of the European Union, Luxembourg. doi: 10.2788/2808.

Dunn, P.K., & Smyth, G.K., 1996. Randomized Quantile Residuals. Journal of Computational and Graphical Statistics 5(3): 236–244.

Garnier, S., 2018. Viridis: Default color maps from 'matplotlib'. Retrieved from https://CRAN.R-project.org/package=viridis

Geelhoed, S.C.V., Friedrich, E., Joost, M., Machiels, M.A.M. & Stöber, N., 2018. Gemini T-c: aerial surveys and passive acoustic monitoring of harbour porpoises 2015. Wageningen Marine Research report C020/17.

Gill, A., Gloyne-Philips, I., Kimber, J. & Sigray, P., 2014. Marine Renewable Energy, Electromagnetic (EM) Fields and EM-Sensitive Animals. In: Shields M. & Payne A. (eds) Marine Renewable Energy Technology and Environmental Interactions. Humanity and the Sea. Springer, Dordrecht. https://doi.org/10.1007/978-94-017-8002-5_6

Hutchison, Z.L, Gill, A.B., Sigray, P., He, H. & King, J.W., 2020a. Anthropogenic electromagnetic fields (EMF) influence the behaviour of bottom-dwelling marine species. *Sci. Rep.*, vol. 10(1): 4219. 2020

Hutchison, Z.L., Secor, D.H. & Gill, A.B., 2020b. The Interaction Between Resource Species and Electromagnetic Fields Associated with Electricity Production by Offshore Wind Farms. Oceanography 33(4): 96–107. https://www.jstor.org/stable/26965753

De Jong C.A.F., Lam, F.P.A., von Benda-Beckmann, A.M., Oud, T.S., Geelhoed, S.C.V., Vallina, T, Wilkes, T. Brinkkemper, J. Snoek, R., in prep. Analysis of the effects on harbour porpoises from the underwater sound during the construction of the Borssele and Gemini offshore wind farms.

Kirschvink, J.L., 1990. Geomagnetic sensitivity in cetaceans: an update with live stranding records in the United States. In Thomas J.A. & Kastelein R.A. (eds). Sensory abilities of cetaceans: laboratory and field evidence. (pp. 639-649). Springer, Boston, MA.

Lazaridis, E., 2014. Lunar: Lunar phase & distance, seasons and other environmental factors. Retrieved from http://statistics.lazaridis.eu

Macaulay, J., Gordon, J., Gillespie, D., Malinka, C. & Northridge, S., 2017. Passive acoustic methods for fine-scale tracking of harbour porpoises in tidal rapids. Journal of the Acoustical Society of America 141: 1120−1132.

R Core Team, 2020. R: A language and environment for statistical computing. Vienna, Austria: R Foundation for Statistical Computing. Retrieved from https://www.R-project.org/

Ramsay, J.O., 1988. Monotone regression splines in action. Statist. Sci. 3(4): 425–441. doi:10.1214/ss/1177012761

Richardson, W.J., Green, C.R.G. jr., Malme, C.I. & Thomson, D.H., 1995. Marine Mammals and Noise. Academic Press, San Diego, 576 pp.

RStudio Team, 2020. RStudio: Integrated development environment for r. Boston, MA: RStudio, PBC. Retrieved from http://www.rstudio.com/

Sakamoto, Y., Ishiguro, M., & Kitagawa, G., 1986. Akaike information criterion statistics. Dordrecht, The Netherlands: D. Reidel 81(10.5555): 26853.

Schaffeld, T., Bräger, S., Gallus, A., Dähne, M. *et al*., 2016 Diel and seasonal patterns in acoustic presence and foraging behaviour of free-ranging harbour porpoises. Mar Ecol Prog Ser 547: 257−272.

Scheidat, M., Bos, O.G., & Geelhoed, S.C.V., 2016. The feasibility of tagging habour porpoises in Dutch waters (Report C009/16). Wageningen Marine Research. https://edepot.wur.nl/370735

Scheidat, M., Geelhoed, S.C.V., & Noort, C.A., 2019. Feasibility of a Passive Acoustic Monitoring (PAM) network for Harbour Porpoises on the Dutch Continental Shelf. (Wageningen Marine Research report; No. C095/19). Wageningen Marine Research. https://doi.org/10.18174/504076

Scheidat, M., Tougaard, J., Brasseur, S., Carstensen, J., van Polanen Petel, T., Teilmann, J. & Reijnders, P., 2011. Harbour porpoises (*Phocoena phocoena*) and wind farms: a case study in the Dutch North Sea. Environ Res Lett 6: 1-10.

Schwarz, G., 1978. Estimating the dimension of a model. The Annals of Statistics: 461–464.

Teilmann J., Akamatsu, T., Miller, L.A., Dietz, R., Tougaard, J. & Siebert, U., 2005. Echolocation behaviour of a wild harbour porpoise during diving. Pp 12-16 In: Abstract Book of the 16th Biennal Conference On The Biology of Marine Mammals, San Diego, California.

Teilmann, J., Christiansen, C.T., Kjellerup, S., Dietz, R. & Nachman, G., 2013. Geographic, seasonal, and diurnal surface behavior of harbor porpoises. Marine Mammal Science 29(2): E60–E76.

Thomsen, F., Gill, A., Kosecka, M., Andersson, M., André, M., Degraer, S., Folegot, T., Gabriel, J., Judd, A., Neumann, T., Norro, A., Risch, D., Sigray, P., Wood, D., Wilson, B., 2015. MaRVEN - Environmental Impacts of Noise, Vibrations and Electromagnetic Emissions from Marine Renewable Energy (Report No. RTD-K3-2012-MRE). Report by Danish Hydraulic Institute (DHI). Report for European Commission.

Tierney, L., 2018. Codetools: Code analysis tools for r. Retrieved from https://CRAN.R-project.org/package=codetools

Tougaard, J., Wright, A.J. & Madsen, P.T., 2015. Cetacean noise criteria revisited in the light of proposed exposure limits for harbour porpoises. Mar. Pollut. Bull. 90 (1-2): 196-208.

Tricas, T.C. &. Carlson, B.A., 2012. Electroreceptors and Magnetoreceptors. In Friedman (ed). Cell Physiology Source Book. Academic Press. Pp 705-725.

Van der Neut, R. & Brinkkemper, J., 2022. EMF and Sound monitoring around the Borssele export cable. Environmental measurements to study effects on harbour porpoise presence. WaterProof Marine Consultancy & Services BV. Report WP1268_R2r0.

Van Polanen Petel, T., Geelhoed, S. & Meesters, E., 2012. Harbour porpoise occurrence in relation to the Prinses Amaliawindpark. IMARES Report number C177/10, IMARES Wageningen UR.

Verfuß, U., Adler, S., Brandecker, A., Dähne, M., Diederichs, A., Gallus, A., Herrmann, A., Krügel, K., Lucke, K., Teilmann, J., Tougaard, J., Tregenza, N., Siebert, U. & Benke, H., 2010. AMPOD: Applications and analysis methods for the deployment of T-PODs in environmental impact studies for wind farms: Comparability and development of standard methods (FKZ 0327587). Final report to the Federal Ministry of the Environment. German Oceanographic Museum, Stralsund.

Verfuß, U.K., Miller, L.A. & Schnitzler, H-U., 2005. Spatial orientation in echolocating harbour porpoises*(Phocoena phocoena*). Journal of Experimental Biology 208: 3385-3394.

Verfuß, U.K., Miller, L.A., Pilz, P.K.D. & Schnitzler, H-U., 2009. Echolocation by two foraging harbour porpoises (*Phocoena phocoena*). Journal of Experimental Biology 212: 823–834.

Vrooman, J., Geelhoed, S.C.V. & Scheidat, M., 2022. Current status of tagging harbour porpoises - application to the Dutch North Sea: Knowledge base report. Wageningen Marine Research report; No. C017/22. Wageningen Marine Research. https://doi.org/10.18174/567532

Wegman, E.J., & Wright, I.W., 1983. Splines in statistics. Journal of the American Statistical Association 78(382): 351–365. Retrieved from http://www.jstor.org/stable/2288640

Wickham, H., 2016. ggplot2: Elegant graphics for data analysis. Springer-Verlag New York. Retrieved from https://ggplot2.tidyverse.org

Wisniewska, D.M., Johnson, M., Teilmann, J., Siebert, U., Galatius, A., Dietz, R., *et al*., 2018. High rates of vessel noise disrupt foraging in wild harbour porpoises (*Phocoena phocoena*). Proc R Soc B, 285(1872):20172314 pmid:2944501

Wood, S.N., 2003. Thin-plate regression splines. Journal of the Royal Statistical Society (B) 65(1): 95–114.

Wood, S.N., 2011. Fast stable restricted maximum likelihood and marginal likelihood estimation of semiparametric generalized linear models. Journal of the Royal Statistical Society (B) 73(1): 3–36.

Wood, S.N., 2017. Generalized additive models: An introduction with r (2nd ed.). Chapman; Hall/CRC.
Wright, A.J., Akamatsu, T., Mouritsen, K.N., Sveegaard, S., Dietz, R. & Teilmann, J., 2017. Silent porpoise: potential sleeping behaviour identified in wild harbour porpoise. Animal Behaviour 133: 211-222.

Xie, Y., 2016. Bookdown: Authoring books and technical documents with R markdown. Boca Raton, Florida: Chapman; Hall/CRC. Retrieved from https://bookdown.org/yihui/bookdown.

IJsseldijk, L.L., Camphuysen, C.J., Nauw, J.J. & Aarts, G., 2015. Going with the flow: tidal influence on the occurrence of the harbour porpoise (*Phocoena phocoena*) in the Marsdiep area. Netherlands Journal of Sea Research 103: 129−137.

Zein, B., Woelfing, B., Dähne, M., Schaffeld, T., Ludwig, S., Hansen Rye, J., Baltzer, J., Ruser, A. & Siebert, U., 2019. Time and tide: Seasonal, diel and tidal rhythms in Wadden Sea Harbour porpoises (*Phocoena phocoena*). PLoS ONE 14(3):e0213348

Appendix: EMF-based coefficient plots

Coefficient plots of the (numerical) covariates for the EMF based Presence/absence model. The plots were made on the linear scale; the y-axis values on the right side show the exponent of the original y-axis values on the left. The solid red line represents the relation between a covariate value (x-axis) and the effect of the covariate value (y-axis). The shaded ribbon gives the 95% confidence interval. When for a range of covariate values the 95% confidence interval touches the horizontal blue dot-dashed line (y=0 and exp(y)=1) on the y-axis, the variable is not relevant for that range of values. The qualitative interpretation is as follows: Higher values of f(x) indicate higher probability for the presence of ppm, lower values indicate lower probability. The quantitative interpretation is as follows: Suppose the covariate $\mathbf{x}$ changes from value $\mathbf{a}$ to value $\mathbf{b}$ and all other covariates do not change, then the odds of the presence of ppm will be multiplied by $\frac{\exp(\mathbf{f(x=b)})}{\exp(\mathbf{f(x=a)})}$. There are 2 sets of plots shown here. Set A shows the main covariates (EMF*locationgroup), and set B the other covariates.

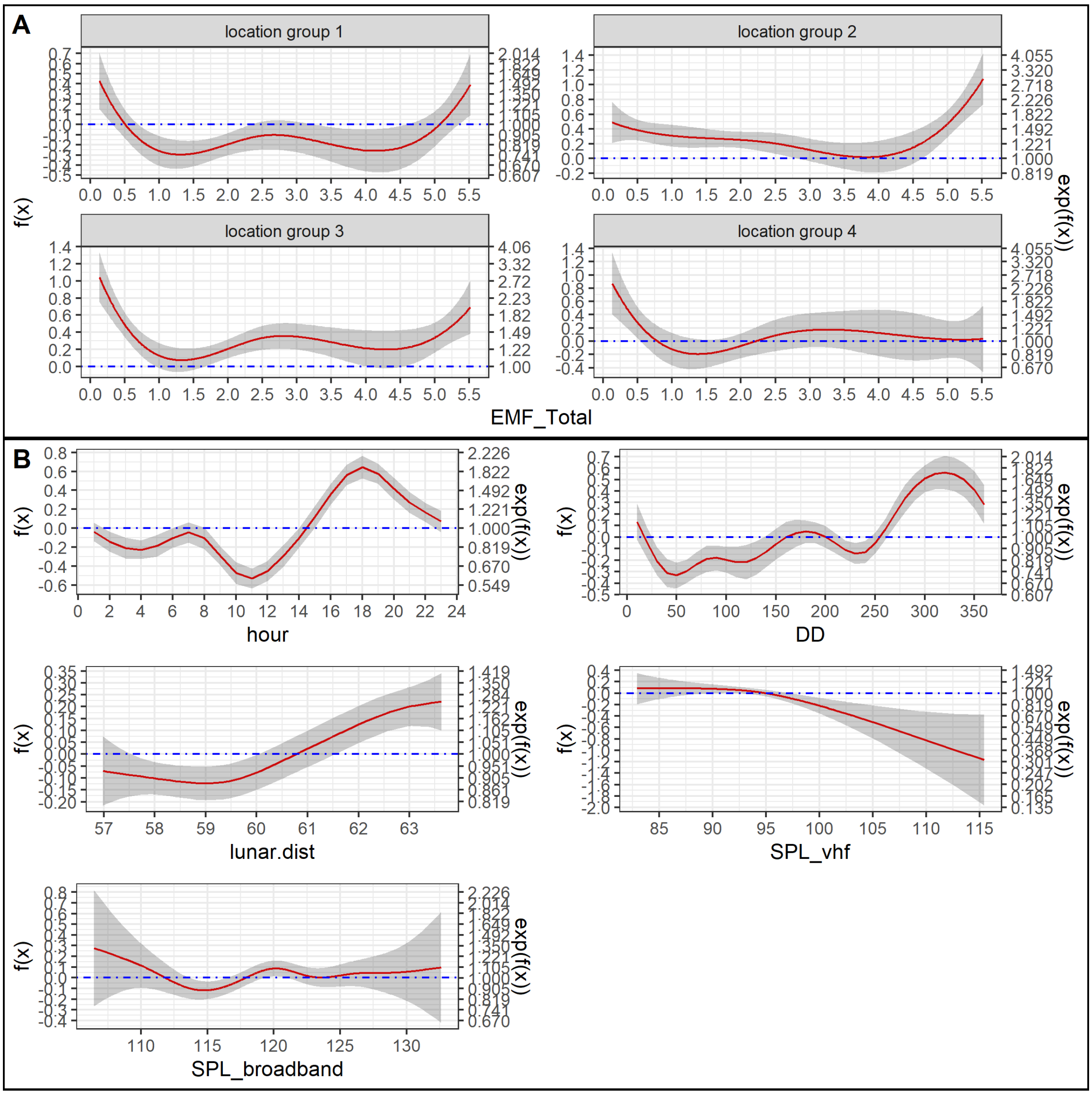

Coefficient plots of the (numerical) covariates for the EMF based non-zero model. The plots were made on the linear scale; the y-axis values on the right side show the exponent of the original y-axis values on the left. The solid red lines represents the relation between a covariate value (x-axis) and the effect of the covariate value (y-axis). The shaded ribbon gives the 95% confidence interval. When for a range of covariate values the 95% confidence interval touches the horizontal blue dot-dashed line (y=0 and exp(y)=1) on the y-axis, the variable is not relevant for that range of values. The qualitative interpretation is as follows: Higher values of f(x) indicate higher expected counts of ppm, lower values indicate lower counts. The quantitative interpretation is as follows: Suppose the covariate $\mathbf{x}$ changes from value $\mathbf{a}$ to value $\mathbf{b}$ and all other covariates do not change, then the ratio $\frac{\text{ppm}}{\mathbf{60}-\text{ppm}}$ will be multiplied by $\frac{\exp(\mathbf{f(x=b)})}{\exp(\mathbf{f(x=a)})}$. There are 2 sets of plots shown here. Set A shows the main covariates (EMF*locationgroup), and set B the other covariates.

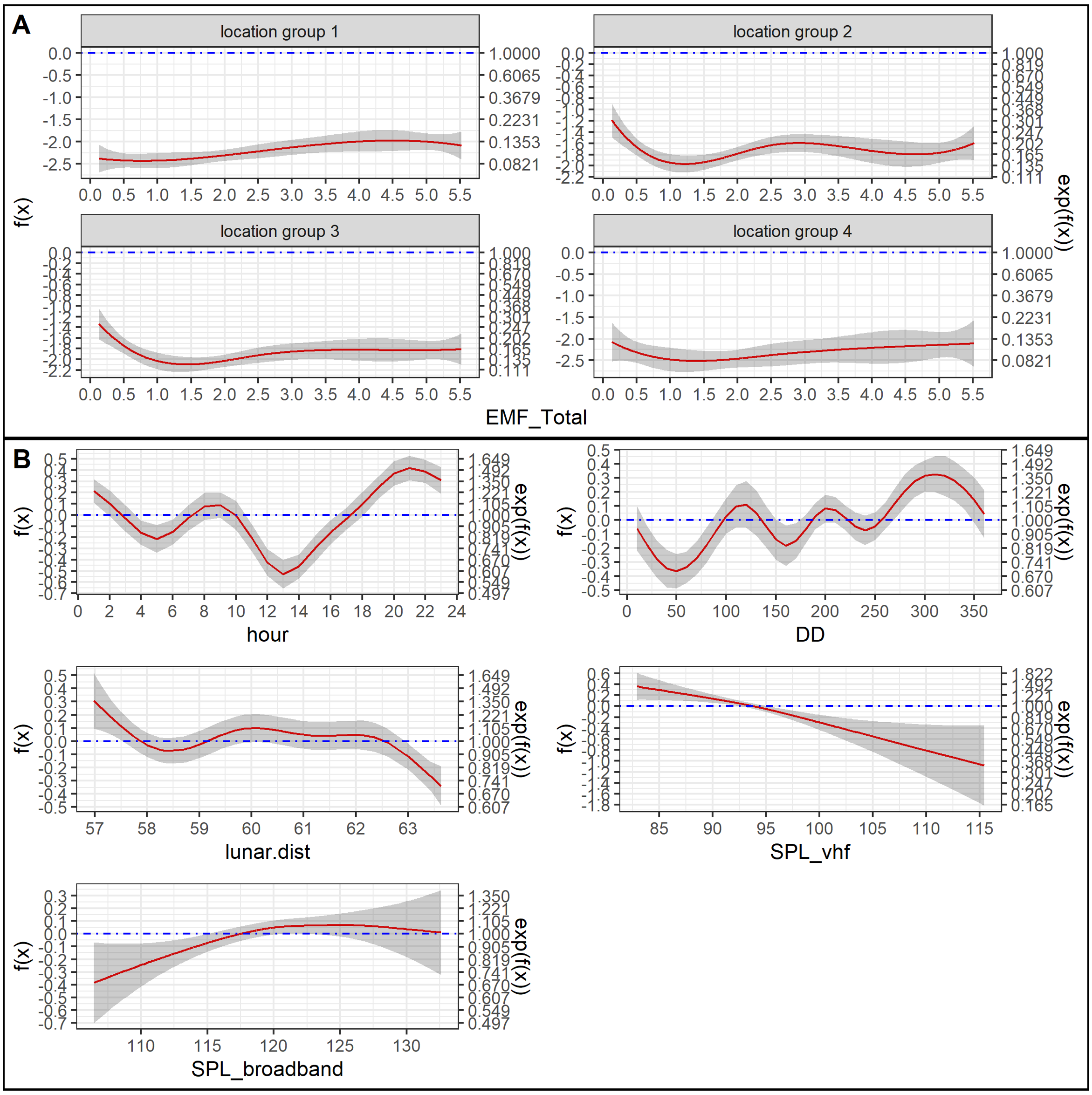

Appendix: wind-based coefficient plots

Coefficient plot of the location group covariate for the wind based Presence/absence model. The plots were made on the linear scale; the y-axis values on the right side show the exponent of the original y-axis values on the left. The black points represent the relation between a covariate value (x-axis) and the effect of the covariate value (y-axis). The red error bars give the 95% confidence interval. When the error bars of one group does not overlap the mean value of the other group and vice-versa, the 2 groups can be said to be significantly different. The qualitative interpretation is as follows: Higher values of f(x) indicate higher probability for the presence of ppm, lower values indicate lower probability. The quantitative interpretation is as follows: Suppose the location group changes from group $\mathbf{a}$ to group $\mathbf{b}$, and all other covariates do not change, then the odds of the presence of ppm will be multiplied by $\frac{\exp(\mathbf{f(x=b)})}{\exp(\mathbf{f(x=a)})}$.

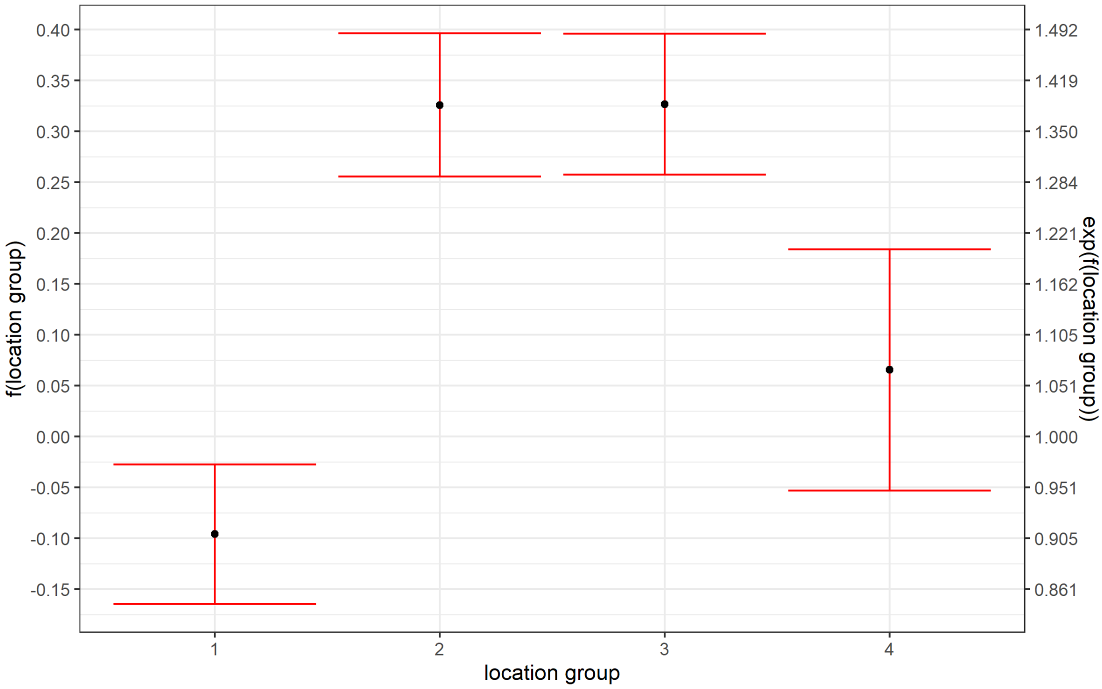

Coefficient plots of the (numerical) covariates for the wind based Presence/absence model. The plots were made on the linear scale; the y-axis values on the right side show the exponent of the original y-axis values on the left. The solid red line represents the relation between a covariate value (x-axis) and the effect of the covariate value (y-axis). The shaded ribbon gives the 95% confidence interval. When for a range of covariate values the 95% confidence interval touches the horizontal blue dot-dashed line (y=0 and exp(y)=1) on the y-axis, the variable is not relevant for that range of values. The qualitative interpretation is as follows: Higher values of f(x) indicate higher probability for the presence of ppm, lower values indicate lower probability. The quantitative interpretation is as follows: Suppose the covariate $\mathbf{x}$ changes from value $\mathbf{a}$ to value $\mathbf{b}$ and all other covariates do not change, then the odds of the presence of ppm will be multiplied by $\frac{\exp(f(x=b))}{\exp(f(x=a))}$.

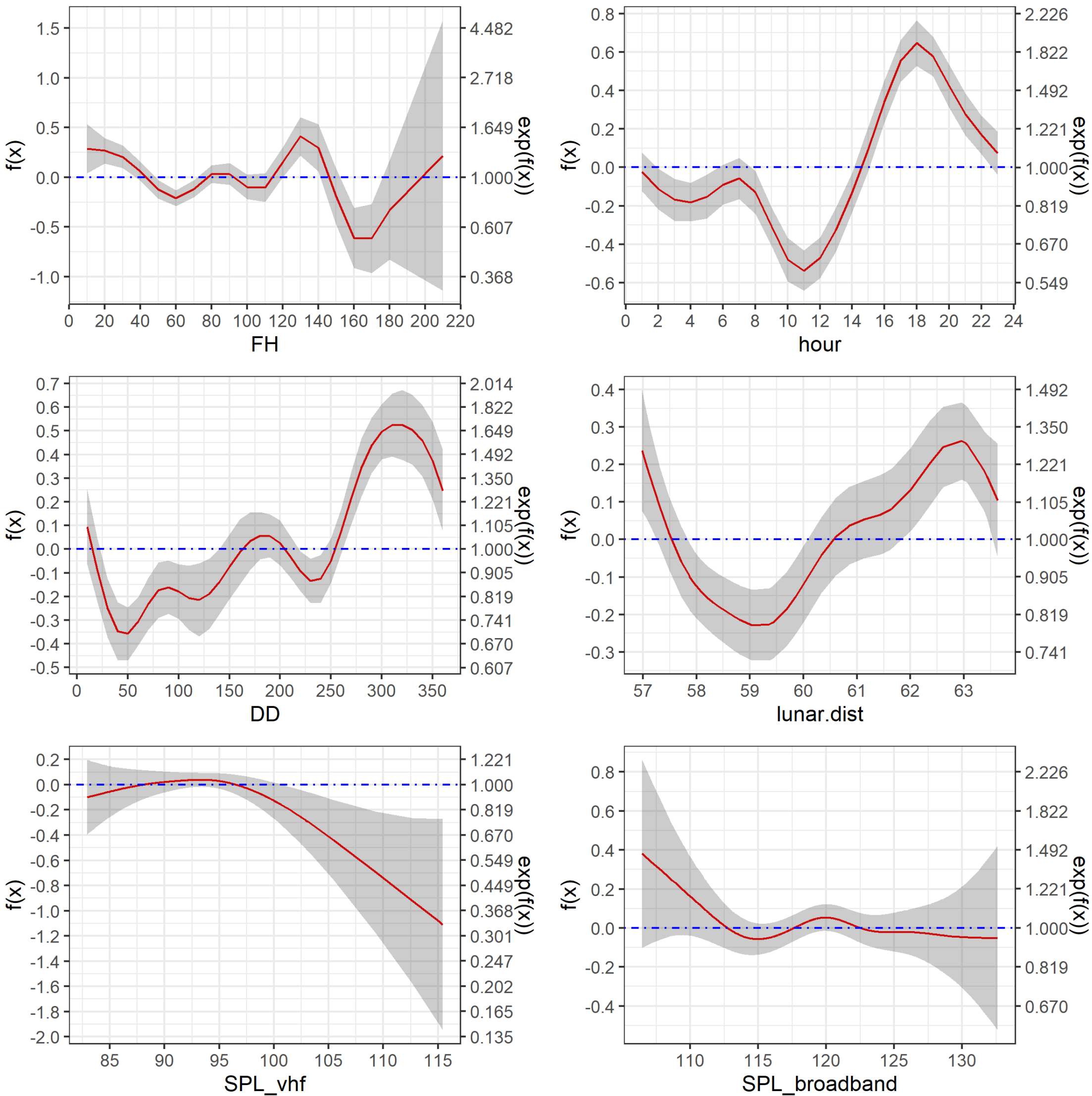

Coefficient plot of the location group covariate for the wind based non-zero model. The plots were made on the linear scale; the y-axis values on the right side show the exponent of the original y-axis values on the left. The black points represent the relation between a covariate value (x-axis) and the effect of the covariate value (y-axis). The red error bars give the 95% confidence interval. When the error bars of one group does not overlap the mean value of the other group and vice-versa, the 2 groups can be said to be significantly different. The qualitative interpretation is as follows: Higher values of f(x) indicate higher probability for the presence of ppm, lower values indicate lower probability. The quantitative interpretation is as follows: Suppose the location group changes from group $\mathbf{a}$ to group $\mathbf{b}$, and all other covariates do not change, then the ratio $\frac{\text{ppm}}{\mathbf{60}-\text{ppm}}$ will be multiplied by $\frac{\exp(\mathbf{f(x=b)})}{\exp(\mathbf{f(x=a)})}$.

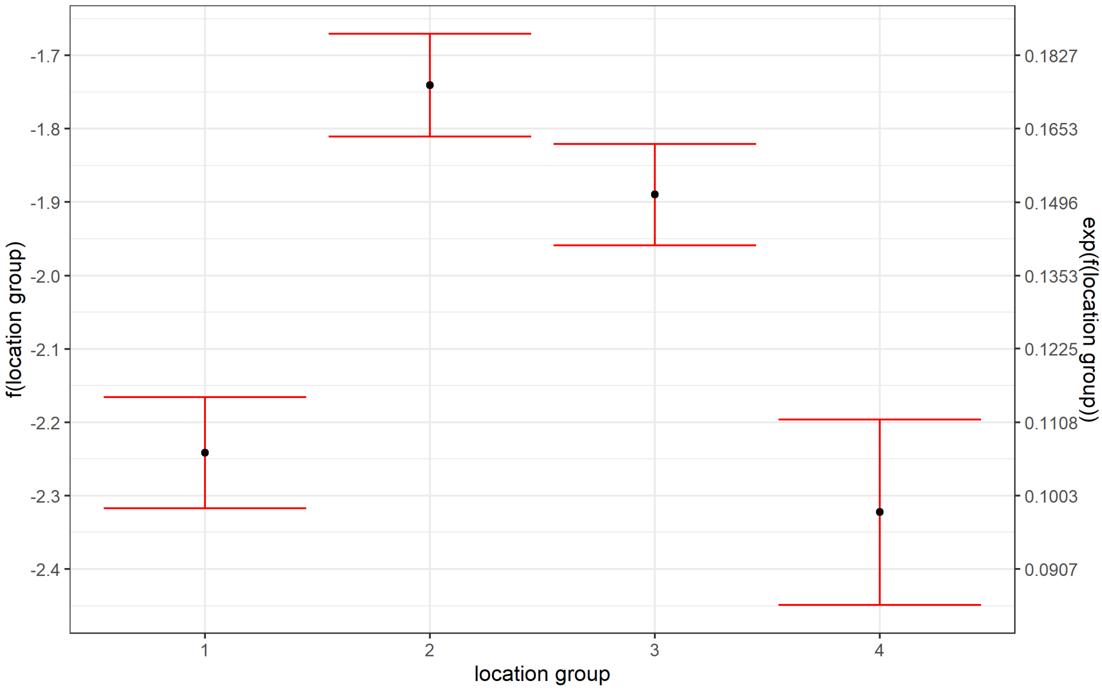

Coefficient plots of the (numerical) covariates for the wind based non-zero model. The plots were made on the linear scale; the y-axis values on the right side show the exponent of the original y-axis values on the left. The solid red lines represents the relation between a covariate value (x-axis) and the effect of the covariate value (y-axis). The shaded ribbon gives the 95% confidence interval. When for a range of covariate values the 95% confidence interval touches the horizontal blue dot-dashed line (y=0 and exp(y)=1) on the y-axis, the variable is not relevant for that range of values. The qualitative interpretation is as follows: Higher values of f(x) indicate higher expected counts of ppm, lower values indicate lower counts. The quantitative interpretation is as follows: Suppose the covariate $\mathbf{x}$ changes from value $\mathbf{a}$ to value $\mathbf{b}$ and all other covariates do not change, then the ratio $\frac{\text{ppm}}{\mathbf{60}-\text{ppm}}$ will be multiplied by $\frac{\exp(\mathbf{f}(\mathbf{x}=\mathbf{b}))}{\exp(\mathbf{f}(\mathbf{x}=\mathbf{a}))}$.

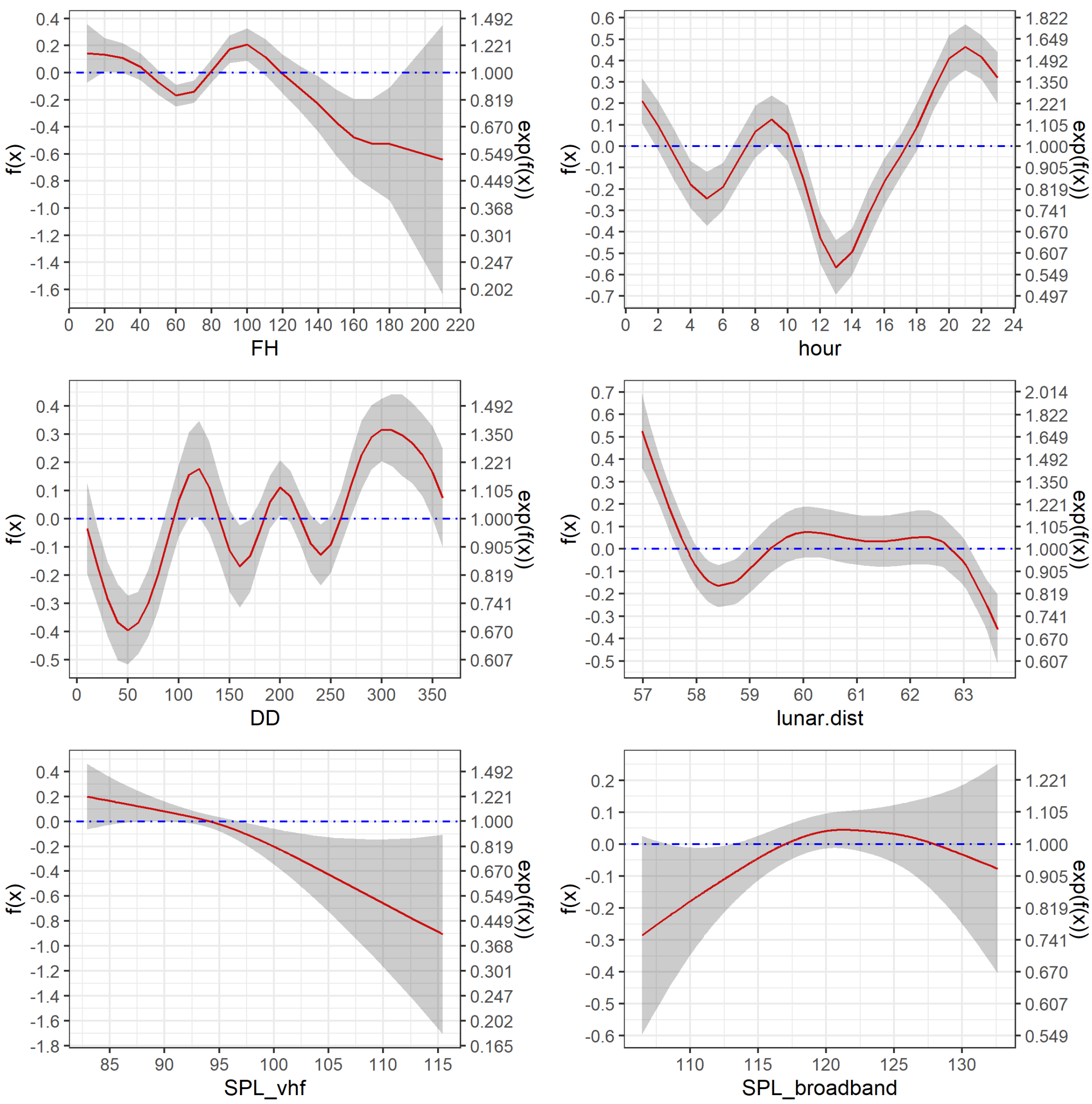

Justification

Report C067/22
Project Number: 4316100259.

The scientific quality of this report has been peer reviewed by a colleague scientist and a member of the Management Team of Wageningen Marine Research

Approved: Erwin Winter
Researcher

Signature:

Date: 28/10/2022

Approved: Drs. Jakob Asjes
MT member Integration

Signature:

Date: 28/10/2022

Wageningen Marine Research
T +31 (0)317 48 7000
E: marine-research@wur.nl
www.wur.eu/marine-research

Visitors' address
- Ankerpark 27 1781 AG Den Helder
- Korringaweg 7, 4401 NT Yerseke
- Haringkade 1, 1976 CP IJmuiden

With knowledge, independent scientific research and advice, **Wageningen Marine Research** substantially contributes to more sustainable and more careful management, use and protection of natural riches in marine, coastal and freshwater areas.

Wageningen Marine Research is part of Wageningen University & Research. Wageningen University & Research is the collaboration between Wageningen University and the Wageningen Research Foundation and its mission is: 'To explore the potential for improving the quality of life'